Electronic Supplementary Material (ESI) for Nanoscale.

Supplementary Information

Quantifying interfacial tensions of surface nanobubbles: How far can Young's equation explain?

Hideaki Teshima*[a,b], Hiroki Kusudo[c], Carlos Bistafa[c], Yasutaka Yamaguchi[c,d]

[a.] Department of Aeronautics and Astronautics, Kyushu University, Nishi-Ku, Motooka 744, Fukuoka 819-0395, Japan

[b.] International Institute for Carbon-Neutral Energy Research (WPI-I2CNER), Kyushu University, Nishi-Ku, Motooka 744, Fukuoka 819-0395, Japan

[c.] Department of Mechanical Engineering, Osaka University, 2-1 Yamadaoka, Suita, 565-0871, Japan

[d.] Water Frontier Research Center (WaTUS), Tokyo University of Science, Shinjuku-Ku, Kagurazaka 1-3, 162-8601, Japan

* Author to whom correspondence should be addressed: hteshima05@aero.kyushu-u.ac.jp

Normal stress profiles under surface nanobubbles

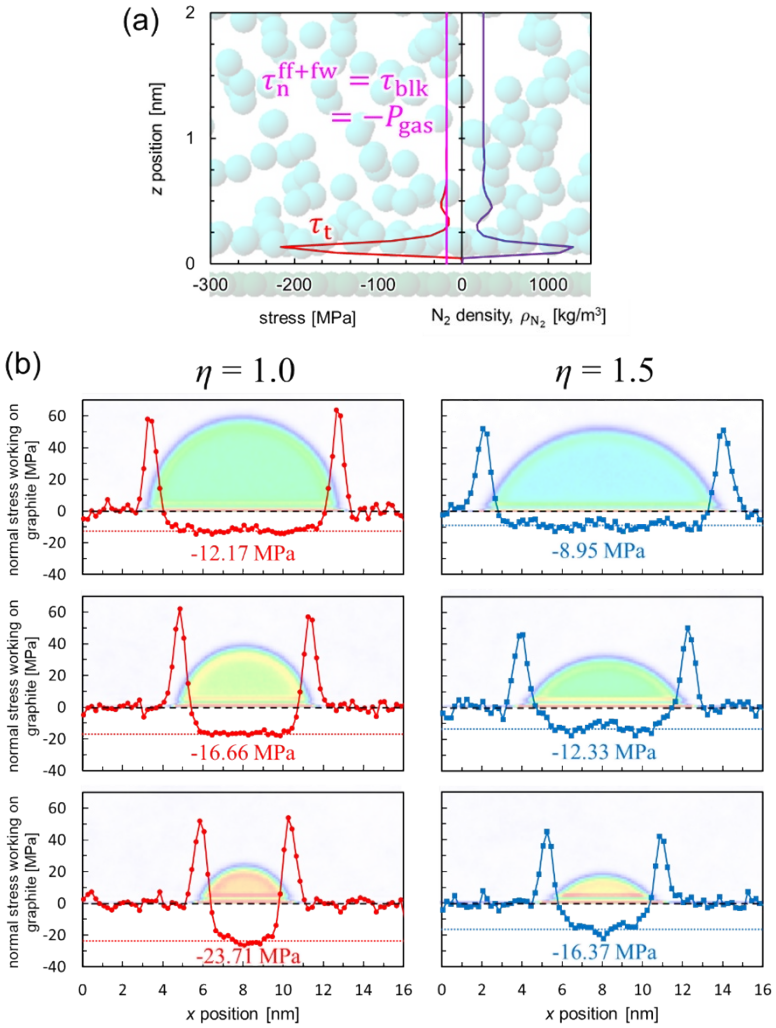

Fig. S1 (a) Distribution of (left) the stress tangential to and normal to the solid-gas interface $\tau_t(z)$ and $\tau^{ff+fw}_n(z)$, where the fluid-fluid and fluid-wall interactions are denoted by the subscripts "ff" and "fw" respectively, and (right) the N_2 density ρ_{N_2}. $\tau_t(z)$ shows correlations with the distribution of ρ_{N_2}, while $\tau^{ff+fw}_n(z)$ is independent of that and a constant equivalent to the bulk stress τ_{blk}, namely the bulk gas pressure with inverted sign ($-P_{gas}$), even inside the adsorbed layers. Therefore, the internal pressure of surface nanobubbles can be estimated from the normal stress working on the graphite. These distributions correspond to the system for the water-N_2 molecule interfacial tension with $N_{N_2} = 200$ for $\eta = 1.0$ shown in Fig. S10(b). Here, the origin of the vertical axis is defined as the position where $\tau_t(z)$ starts to have non-zero values. (b) Profiles of the

normal stress working on the bottom graphite in the cases of (left column) η = 1.0 and (right column) η = 1.5. Nanobubbles are composed of N_{N_2} = 400, 250, and 150 (from the top). The average stress under the nanobubble is assumed as the pressure with inverted sign $-P_{gas}$.

Peak density of gas molecules inside N_2 molecule-adsorbed layers

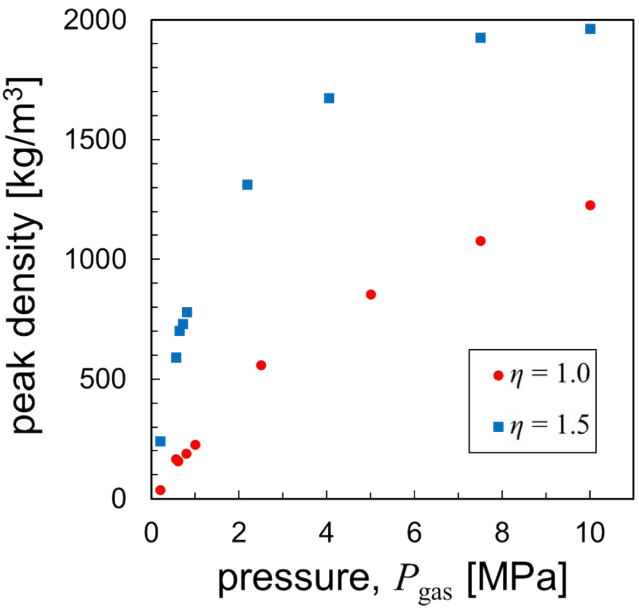

Fig. S2 Peak density inside N_2-adsorbed layers under surface nanobubbles vs. the corresponding pressure P_{gas}. Circle (red) and square (blue) points correspond to the results of η = 1.0 and 1.5, respectively.

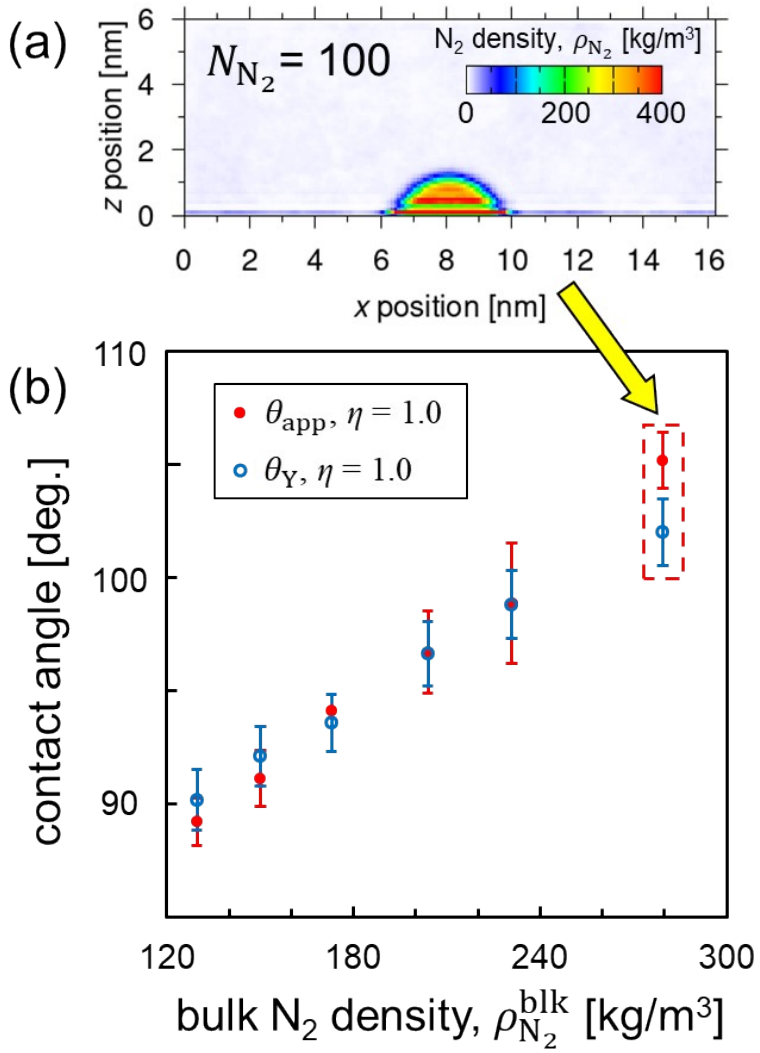

Breakdown of Young's equation for the case of N_{N_2} = 100 and η = 1.0.

Fig. S3 (a) Density distribution of a nanobubble with N_{N_2} = 100 and η = 1.0 and (b) contact angles of θ_Y and θ_{app} estimated by Young's equation (Eq. (1) in the main manuscript) and apparent shape of the nanobubbles for the cases of N_{N_2} = 400, 300, 250, 200, 150, and 100 with η = 1.0.

Calculation of the contact angles of semispherical submicron-sized bubbles

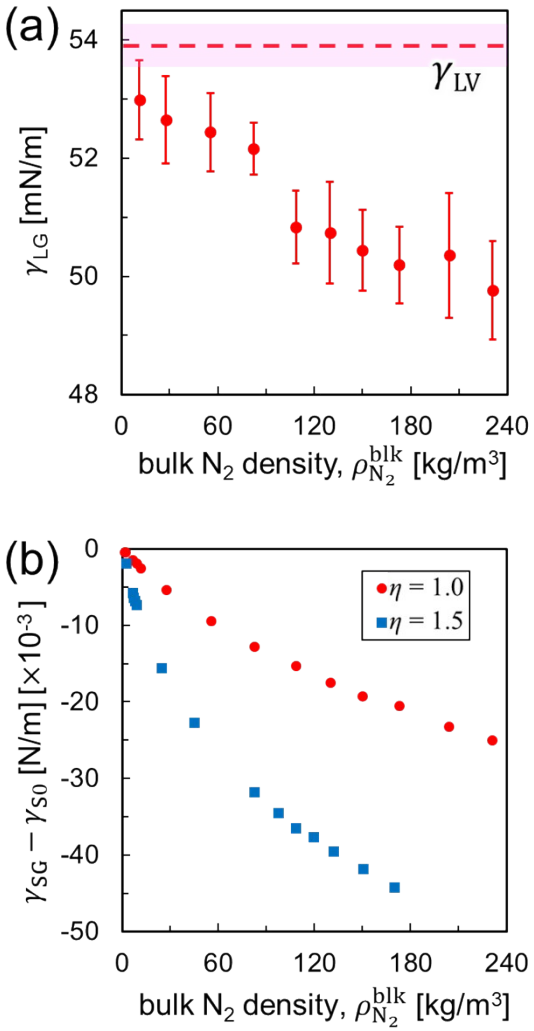

Fig. S4 (a) γ_{LG} and (b) $\gamma_{SG} - \gamma_{S0}$ as a function of a wide range of bulk N_2 density values $\rho_{N_2}^{blk}$. Circle (red) and square (blue) points correspond to the results of η = 1.0 and 1.5, respectively. The red dashed line indicates the value of $\gamma_{LV} = 53.9 \pm 0.4 \times 10^{-3}$ N/m.

To estimate the contact angles θ_Y of the submicron-sized nanobubbles, we calculated $\gamma_{SG} - \gamma_{S0}$ for a wide range of the pressure P_{gas} (shown in Figure 4(a) in the main manuscript) and corresponding bulk N_2 density $\rho_{N_2}^{blk}$ (Figure S4(b)) by using the system shown in Figure S10(b). We can see that $\gamma_{SG} - \gamma_{S0}$ approaches zero as $\rho_{N_2}^{blk}$ decreases for

both η = 1.0 and 1.5. By substituting γ_{LG} and $\gamma_{SG} - \gamma_{S0}$ for a wide range of $\rho_{N_2}^{blk}$ (Figure S4(a, b)) into Eq. (1) in the main manuscript, plots of θ_Y as functions of $\rho_{N_2}^{blk}$ and corresponding P_{gas} are obtained as shown in Figure S5(a, b).

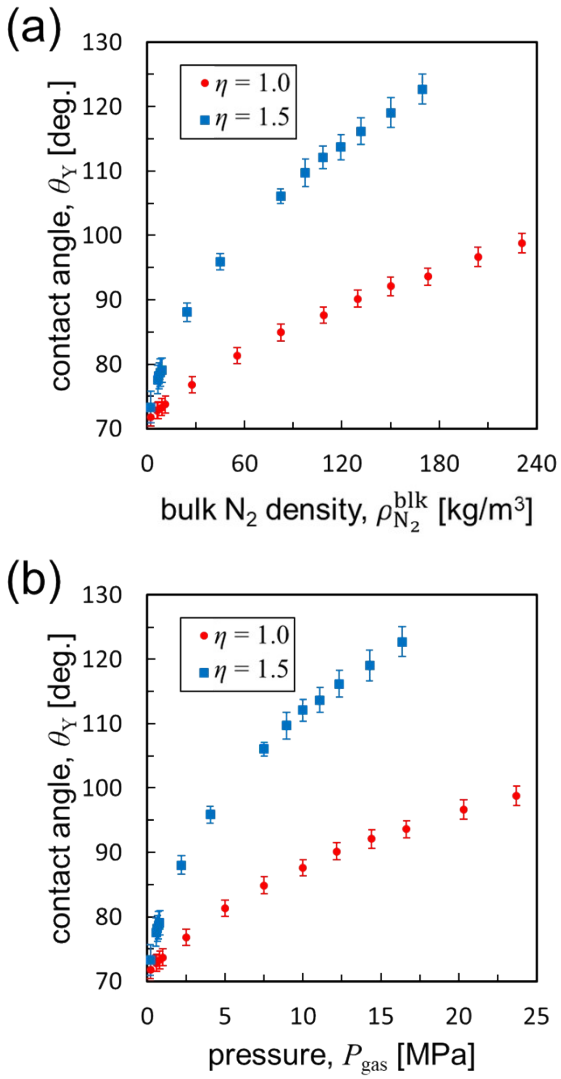

Fig. S5 θ_Y estimated by Eq. (1) in the main manuscript as functions of (a) bulk N_2 density $\rho_{N_2}^{blk}$ and (b) the corresponding pressure P_{gas}. Circle (red) and square (blue) points correspond to the results of η = 1.0 and 1.5, respectively.

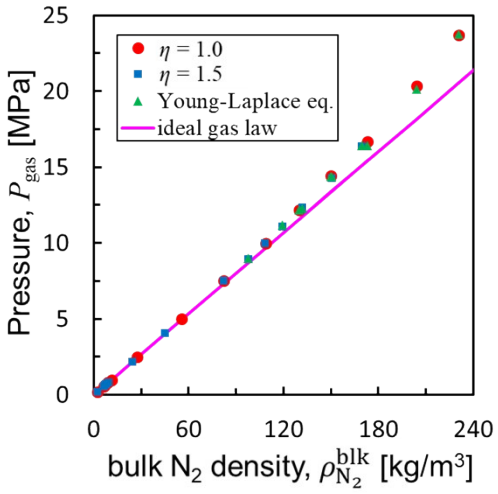

Fig. S6 Pressure P_{gas} vs. the corresponding bulk N_2 density $\rho_{N_2}^{blk}$. Circle (red) and square (blue) points correspond to the pressure of η = 1.0 and 1.5, respectively. Triangle (green) points indicate the pressure obtained by the Young-Laplace equation for quasi-2D nanobubbles $P_{gas} = P_0 + \frac{\gamma_{LG}}{r_{2D}}$. The (pink) line indicates the pressure estimated by ideal

Next, we calculated the radius of curvature of semispherical nanobubbles r_{3D} corresponding to P_{gas}. Figure S6 shows the relationships between P_{gas} and $\rho_{N_2}^{blk}$. As $\rho_{N_2}^{blk}$ increases, because the frequency of collisions among N_2 molecules increases, the deviation of the inner pressure from the ideal gas law $P_{gas} = \rho_{N_2}^{blk} R_{gc} T$ becomes large. Here $R_{gc} = 296.8$ J/(kg*K) is a gas constant for nitrogen. In contrast, the pressure calculated through the Young-Laplace equation for quasi-two-dimensional nanobubbles $P_{gas} = P_0 + \frac{\gamma_{LG}}{r_{2D}}$ agreed very well with the pressure of the nanobubbles obtained from the normal stress working on the bottom graphite (shown in Figure S1). Here, r_{2D} was calculated by least-squares circular fitting to a contour of the liquid-gas interface. Therefore, it can be considered that the Young-Laplace equation is applicable to surface nanobubbles with a wide range of size.

Thus, by applying the Young-Laplace equation for semispherical nanobubbles $P_{gas} = P_0 + \frac{\gamma_{LG}}{r_{3D}}$ and the footprint radius $R_{FP} = r_{3D}\sin\theta_Y$ to the relationship between θ_Y and P_{gas} (Figure S5(b)), we could obtain the relationship between θ_Y and R_{FP} as shown in Figure 4(b) in the main manuscript. Here, the line tension was assumed to be negligible because its typical value is about 10^{-12} to 10^{-10} J/m[1,2] and is sufficiently small.

Bulk N_2 density inside nanobubbles estimated using eqn (4) in the main manuscript

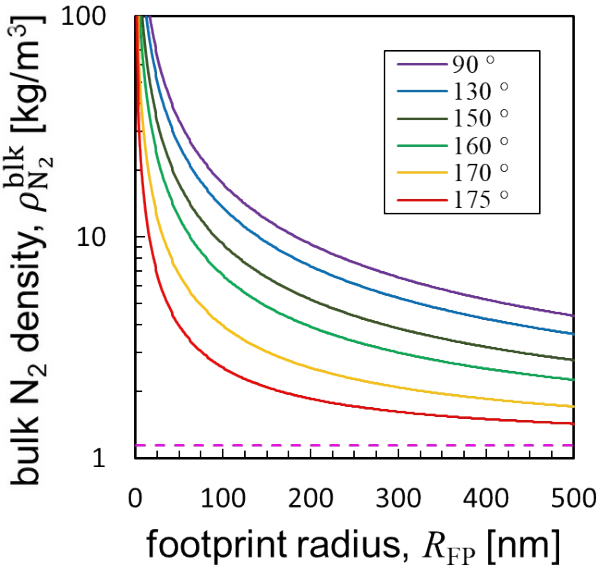

Fig. S7 Bulk N_2 density $\rho_{N_2}^{blk}$ inside nanobubbles estimated by Eq. (4) in the main manuscript as a function of footprint radius R_{FP} for different contact angles. The pink dashed line indicates the nitrogen density under atmospheric pressure (1.14 kg/m^3). The gas density with a contact angle of 90° corresponds to that inside bulk nanobubbles, in which the footprint radius in the horizontal axis is read as the radius of curvature.

Density distributions of N_2 molecules in nanobubble systems

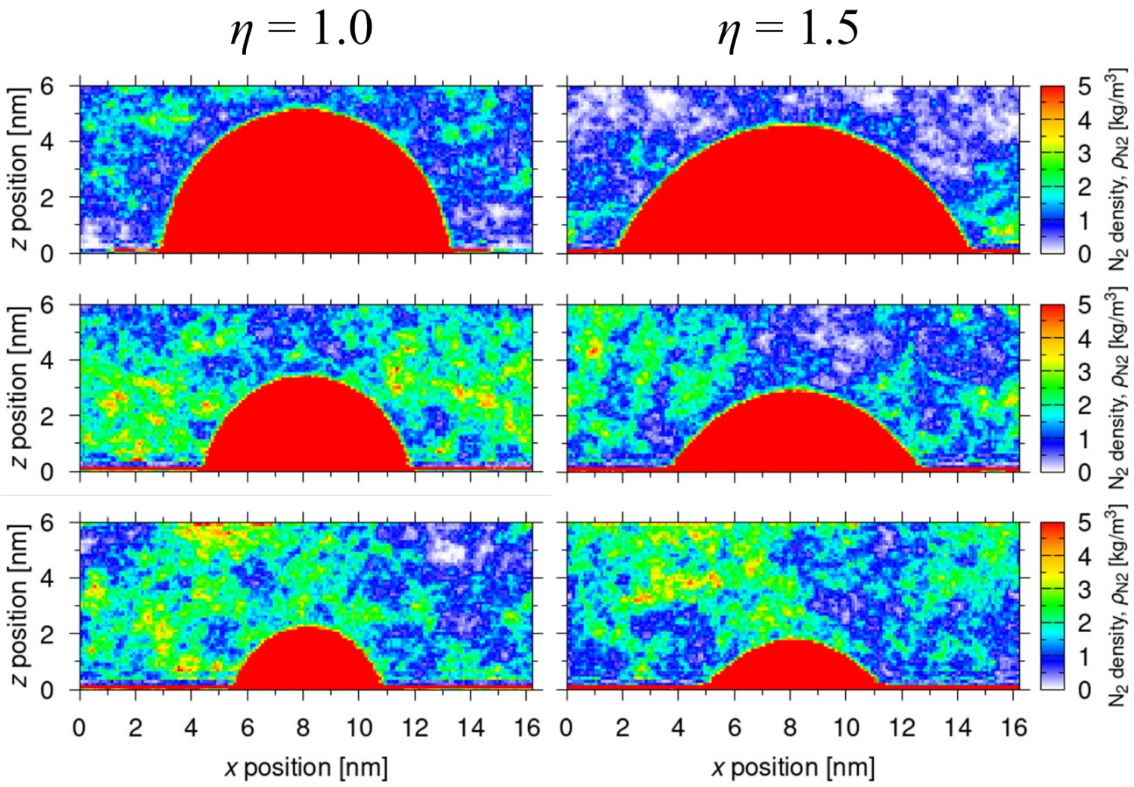

Fig. S8 Density distributions of N_2 molecules with a small range of N_2 density in the cases of N_{N_2}= 400, 250, and 150 (from the top) with (left column) η = 1.0 and (right column) 1.5. In all cases, the dissolved N_2 concentration is above 1.0 kg/m^3 almost in all regions.

Density distributions of water molecules in nanobubble systems

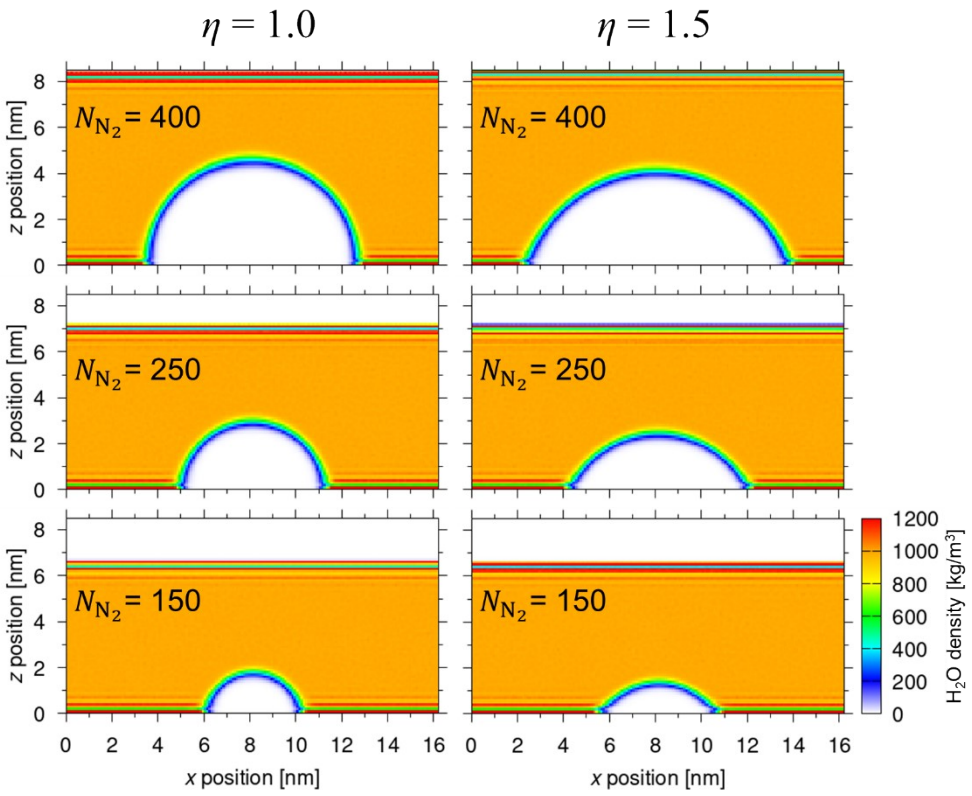

Fig. S9 Density distributions of water in the systems of N_{N_2} = 400, 250, and 150 (from the top) with η = 1.0 and 1.5.

Systems used for the calculation of interfacial tensions

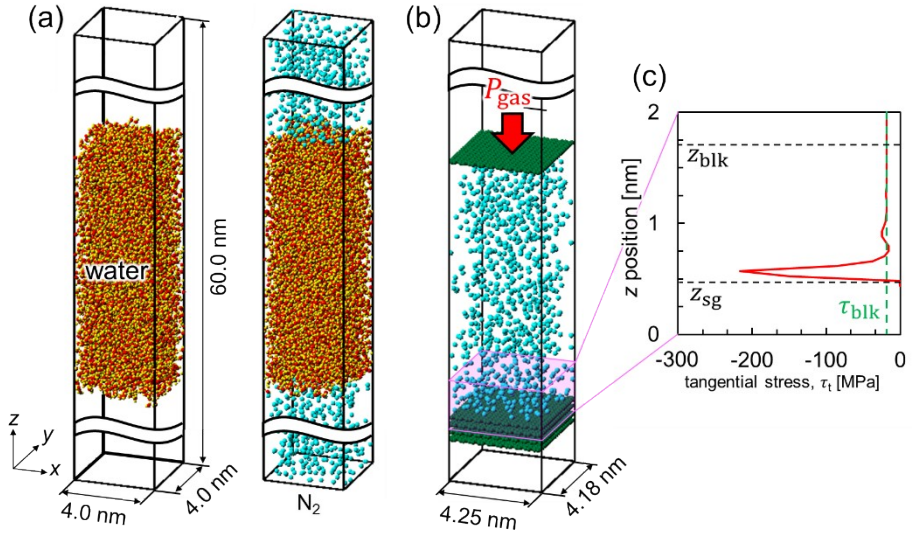

Fig. S10 (a) Simulation systems for the calculation of (left) the water-vapor and (right) the water-N_2 molecule interfacial tensions γ_{LV} and γ_{LG}, respectively. The z-length of the right system was controlled to give the corresponding N_2 density. (b) Simulation system for the calculation of the solid-gas interfacial tension relative to the solid-vacuum interfacial tension $\gamma_{SG} - \gamma_{S0}$. Time average was taken for 20 ns after 10 ns equilibration in the systems of (a) and 100 ns after 150 ns equilibration in the systems of (b). (c) Distribution of the fluid stress tangential to the solid/gas interface $\tau_t(z)$, where green dashed line indicates $\tau_{blk} = - P_{gas}$.

In the first system of Figure S10(a), 5300 water molecules were confined in a simulation cell of 4.0 × 4.0 × 60.0 nm^3 with the periodic boundary condition imposed in all directions. In the second system, 5300 water and 2200-3900 N_2 molecules were confined. Here, the Nosé–Hoover barostat was used to keep the average surface normal pressure in the z-direction P_{zz} at the same value of the pressure inside surface nanobubbles P_{gas} that was obtained in Figure S1, i.e., the N_2 density in the system should be the same as that of the nanobubbles.

In the system of Figure S10(b), the carbon atoms constituting the graphite were fixed onto the space, while the upper graphene worked as a piston to control the system pressure. By applying the same pressures as that inside the nanobubbles P_{gas}, the graphite-N_2 interfaces similar to the ones under the nanobubbles were constructed. The distributions of the fluid stress tangential to the solid-gas interface $\tau_t(z)$ and bulk stress τ_{blk} as a function of the normal position z near the solid-gas interface in the case of N_{N_2} = 200 for η = 1.0 is shown in Figure S10(c) as an example.

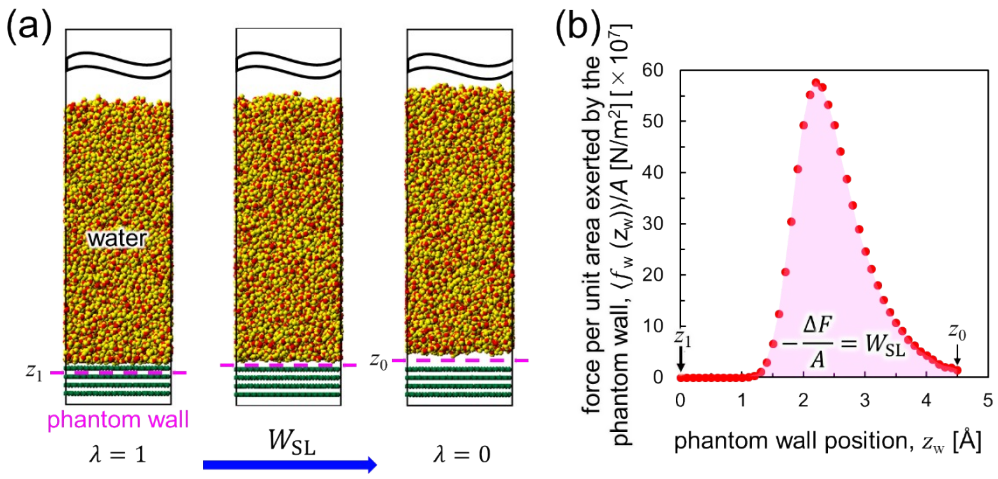

Fig. S11 (a) Schematics of the TI for the calculation of the solid-liquid work of adhesion W_{SL}. 6000 water molecules were put on the graphite in a simulation cell of 4.18 × 4.25 × 20.0 nm^3. Pink dashed line represents the positions of phantom wall repulsively interacting only with the water molecules. The periodic boundary conditions were employed in the horizontal directions. Time average was taken for 0.5 ns after 0.1 ns equilibration for each system. (b) Force per unit area exerted by the phantom wall on liquid $\langle f_w(z_w)\rangle/A$. The pink area corresponds to the quantitative value of the solid-liquid work of adhesion $W_{SL} = 71.2 \pm 0.6 \times 10^{-3}$ N/m.

Supplemental References

1 H. Zhang, S. Chen, Z. Guo, Y. Liu, F. Bresme and X. Zhang, *J. Phys. Chem. C*, 2018, **122**, 17184–17189.

2 N. Kameda, N. Sogoshi and S. Nakabayashi, *Surf. Sci.*, 2008, **602**, 1579–1584.